Sensors & Actuators: B. Chemical 283 (2019) 182–187

Contents lists available at ScienceDirect

Sensors and Actuators B: Chemical

journal homepage: www.elsevier.com/locate/snb

Rapid and sensitive detection of formaldehyde using portable 2-dimensional gas chromatography equipped with photoionization detectors

Hongbo Zhu[a,b], Jinyan She[a,b], Menglian Zhou[a,b], Xudong Fan[a,b,*]

[a] Department of Biomedical Engineering, University of Michigan, 1101 Beal Avenue, Ann Arbor, MI, 48109, United States
[b] Center for Wireless Integrated MicroSensing and Systems (WIMS^2), University of Michigan, Ann Arbor, MI, 48109, United States

ARTICLE INFO

Keywords:
Gas chromatography
2D GC
Formaldehyde detection
Photoionization detector
Air quality control
Indoor air analysis

ABSTRACT

We developed an automated and highly portable device for rapid and sensitive formaldehyde detection based on heart-cutting 2-dimensional gas chromatography. In this design, the air sample was first absorbed by a pre-concentrator before it is injected into the 1st-dimensional column (Rtx®-VMS). The partial elution from the 1st-dimensional column containing formaldehyde was re-injected into the 2nd-dimensional column (Rt® Q-BOND column) for further separation. The detection of formaldehyde was achieved by using a micro-helium dielectric barrier discharge photoionization detector that is able to ionize formaldehyde (ionization potential = 10.88 eV). Due to the use of many miniaturized components, the entire system has a weight of only 1.3 kg (excluding the helium cartridge) and dimensions of only 27 cm x 24 cm x 12 cm. It is capable of detecting formaldehyde down to 0.5 ppb (V/V) with a signal-to-noise ratio of 6 in only 11 min (including 6 min of sampling). Meanwhile, simultaneous separation and detection of other air pollution related toxic compounds, such as benzene, toluene, ethylbenzene, and xylene, was also demonstrated by the 1-dimensional column and a flow-through micro-photoionization detector. The device developed here should have a broad range of applications in environmental protection, industries, space exploration, and battlefield.

1. Introduction

Air pollution is known to be a major environmental concern to human health. The indoor air pollution shows even more significant impact due to a higher accumulation level of toxic volatile organic compounds (VOCs) [1]. Formaldehyde is one of the most commonly found polluting VOCs, which may come from smoking, cooking, heating, decoration materials, furniture finishing, and chemical reactions between VOCs and ozone [2]. Formaldehyde can cause many symptoms, such as burning sensations in eyes, nose, and throat, coughing, wheezing, nausea, and skin irritation by short-term exposure [3], and can be carcinogenic by long-term exposure [4]. Therefore, health and environmental organizations (*e.g.*, World Health Organization (WHO), US National Institute for Occupational Safety and Health (NIOSH), and California Air Resources Board) have established regulated exposure limits, which is summarized in Table S1.

To date, a number of analytical methods, such as spectrophotometry [5], high-performance liquid chromatography [6], gas chromatography (GC) coupled with mass spectrometry(GC/MS) [7,8], and fluorimetry [9], have been developed for formaldehyde detection. While accurate and repeatable, the above instruments suffer from bulky size, complicated processes (such as derivatization), and/or inability for real-time on-site measurement. On the other hand, a few portable devices are available for on-site formaldehyde detection. For example, the handheld formaldehyde detector based on an electrochemical thin-film metal oxide sensor has a reasonably good detection limit (down to ppb level) and quick response time (6 s of rise time to reach 90% of the maximum response and 6 s of recovery time to decrease to 10% of the maximum response) [10]. However, because of the poor selectivity, this type of device has high false positives, particularly at high concentrations of VOC background, and requires frequent calibrations. Paper-based colorimetric measurement is simple with the benefit of low cost and user-friendly [11], but it suffers from limited shelf time and imprecise measurement result. To overcome the aforementioned issues, miniaturized spectrophotometers [12–14] and fluorometers [13] have been developed. However, they require manual operation and specific reaction reagents, which is cumbersome and limits their capability to detect multiple VOCs.

In order to provide a better capability of rapid on-site monitoring of air quality, particularly, formaldehyde, we developed an automated miniaturized heart-cutting 2-dimensional (2-D) GC device. In this device, the 1st-dimensional GC column was coupled to the 2nd-

* Corresponding author at: Department of Biomedical Engineering, University of Michigan, 1101 Beal Avenue, Ann Arbor, MI, 48109, United States.
E-mail address: xsfan@umich.edu (X. Fan).

https://doi.org/10.1016/j.snb.2018.11.156
Received 4 June 2018; Received in revised form 28 September 2018; Accepted 28 November 2018
Available online 29 November 2018
0925-4005/

dimensional GC column *via* a micro-Deans switch. A flow-through micro-photoionization detector (μPID) and a micro-helium dielectric barrier discharge photoionization detector (μHDBD-PID) were installed at the end of 1st- and 2nd-dimensional column, respectively. Owning to the high photon energy (up to 17.5 eV) of the μHDBD-PID, formaldehyde, which was cut from the 1st-dimensional column into the 2nd-dimensional column, can be detected directly without complicated derivatization processes used in traditional GC methods, whereas other air quality related VOCs (such as benzene, toluene, ethylbenzene, and xylene) can be separated by the 1st-dimensional column and subsequently detected by the μPID. The device is highly portable, having weight of about 1.3 kg and dimensions of 27 cm x 24 cm x 12 cm, and is capable of detecting formaldehyde down to 0.5 ppb (V/V) with a signal-to-noise ratio of 6 in only 11 min (including 6 min of sampling time).

2. Materials

The analytes and glass beads (212 ~ 300 μm i.d.) used in flow resistor were purchased from Sigma-Aldrich (St. Louis, MO) and used without any post treatment. The adsorbent material Carbopack™ X (P/N 10437-U), Carbopack™ B (P/N 20273), and Carboxen® 1000 (P/N 10478-U) were obtained from Supelco (Bellefonte, PA). The micro two-port (P/N LHDB1252115H) and three-port valves (P/N LHDA1221311H) and K-type thermocouple (P/N SA3-K) were purchased from Lee Company (Westbrook, CT) and Omega Engineering (Stamford, CT), respectively. The capillary GC column Rtx®-VMS (5 m x 0.25 mm i.d., 1.4 μm film thickness), Rt® Q-BOND (3 m x 0.32 mm i.d., 10 μm film thickness), deactivated fused silica capillary (0.53 mm i.d.), and universal quick seal connectors were obtained from Restek (Bellefonte, PA). A data acquisition card, USB-6003 OEM (16 bits), was purchased from National Instruments (Austin, TX). A mini-diaphragm pump was purchased from Parker Hannifin (P/N E134-11-120, Cleveland, OH). The water used in experiment was purified by a Milli-Q water purification system (Thermo Fisher Scientific, Wayne, MI). Ultrapure helium (99.999%) used as auxiliary gas of μHDBD-PID and system carrier gas in all experiments was purchased from Cryogenic Gases (Ann Arbor, MI). Nickel 200 wire (26 AWG) and Nichrome 80 wire (32 AWG) used as a heating wire for the capillary column and preconcentrator, respectively, were purchased from Newegg (Industry, CA).

3. Methods

3.1. System layout

Fig. 1A illustrates the layout of the GC device. It was housed in a plastic box shown in Fig. 1B, which had compact dimensions of 27 cm x 24 cm x 12 cm and weighed around 1.3 kg. A power adapter with the maximum output of 45 W was applied to provide 24 V DC for the entire device. The DC-DC converters and MOSFET modules were integrated on a home-made printed circuit board to power and control electrical components, such as valves, pump, μPID, μHDBD-PID, preconcentrator, thermal injector, and heaters on the GC columns, *etc*. The average power consumption of the entire device was about 25 W. A LabView™ program was developed for automated operation and data processing, including sampling, sample injection, gas flow routing, column temperature control, and data acquisition, processing, and storage.

3.2. Components

3.2.1. GC columns

The columns used in this system were 5 m Rtx®-VMS and 3 m Rt® Q-BOND for the 1st- and 2nd-dimensional separation, respectively. The GC column was wrapped by a heat shrinkable tube along with a Nickel 200 heating resistance wire, and coiled into a single layer helix of 10 cm in diameter. As shown in Fig. 2A, the miniaturization of GC column in this system was achieved by applying a fan-less design. Instead of using the forced air convection heat transfer method with a fan to reduce the column temperature gradient in a conventional GC system, the uniform temperature was achieved by applying a high thermal conductive material (stainless steel foil) to the column coil. In this design, the temperature gradient in the GC column was reduced by increasing heat transfer efficiency in the column coil. The infrared thermal imaging in Fig. S1 shows uniform temperature distribution with a maximal temperature difference of only 3 °C in the column coil. The column temperature programmed control was achieved by a pulse-width-modulated trigger (100 Hz, 5 V square wave) to MOSFET *via* USB-6003 OEM digital output, whereas the column temperature was monitored by a thermocouple embedded in the column coil. The single point temperature measurement *via* a thermocouple can accurately report the column temperature, which, together with an accurate temperature feedback control, helps maintain the stable analyte retention time.

3.2.2. Preconcentrator and thermal injector

The preconcentrator and thermal injector were used to trap/concentrate VOCs at room temperature with adsorption materials, followed by quick injection of the trapped VOCs into the GC column. As shown in Fig. 2B, the preconcentrator consisted of a deactivated fused silica tube (0.53 mm i.d. and 0.69 mm o.d.) filled with three segments of absorption materials (*i.e.*, Carbopack™ B, Carbopack™ X, and Carboxen® 1000 with a weight of 1 mg each) and sealed with a segment of copper wire on each end. A Nichrome 80 wire with a resistance of 18 Ω was wrapped tightly around the outer wall of the tube. In order to enhance thermal conductivity in the section of adsorption material, a 2 cm long helix copper wire was inserted into the tube. The thermal injector was the same as the preconcentrator in all aspects, except that only 1 mg of Carboxen® 1000 was used as the adsorption material, since it was designed to trap highly volatile compounds such as formaldehyde. The preconcentrator (or thermal injector) was preconditioned at 300 °C for

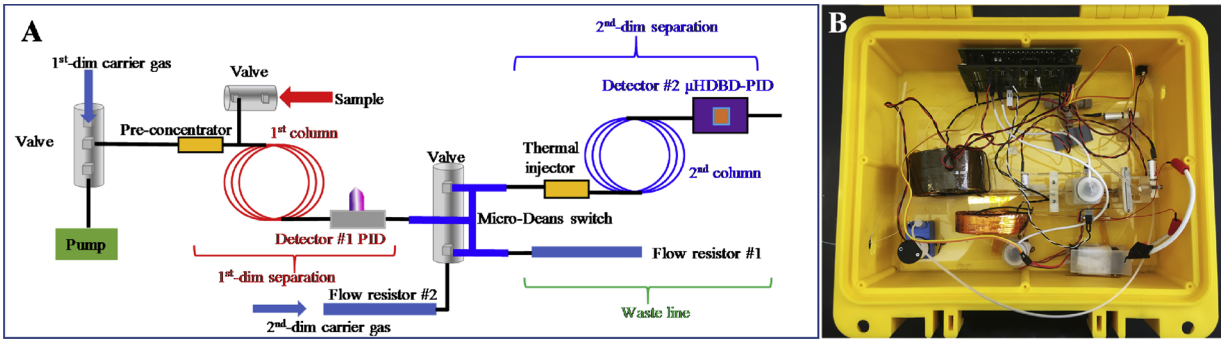

Fig. 1. (A) Layout of the portable 2-D heart cutting GC device. (B) Picture of the device housed in a plastic box of 27 cm x 24 cm x 12 cm. It weighed 1.3 kg, excluding the small helium cartridge.

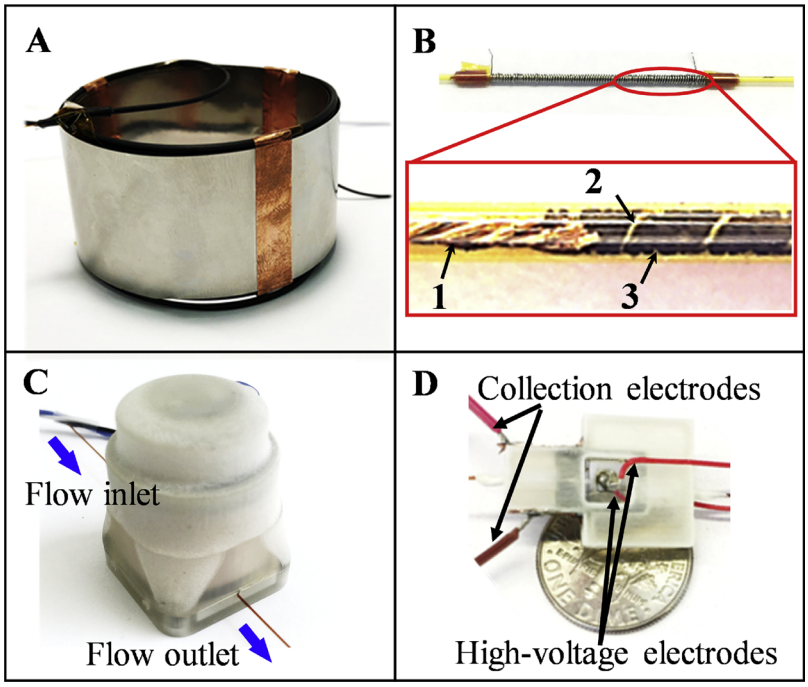

Fig. 2. (A) Picture of an Rtx®-VMS 5 m long GC column coil packaged in a stainless steel foil. (B) Picture of a preconcentrator. The enlarged portion shows the (1) sealing wire, (2) internal helix copper wire, and (3) adsorption material (Carbopack™ B beads) (C) Picture of a μPID packaged in a 3D printed case with a section of guard column (250 μm i.d.) connected on each side. (D) Assembled μHDBD-PID with signal collection electrodes and high-voltage electrodes.

12 h under helium flow before installed in the system. During the operation, in order to generate a sharp injection, 24 V DC was applied to the heating wire for 0.5 s to rapidly heat the preconcentrator (or thermal injector) to 300 °C. Subsequently, a 10% pulse-width-modulated 24 V DC was applied to heat the device continuously and maintain the temperature at 300 °C for 7.5 s in order to completely desorb VOCs. Owing to the low thermal mass design, the total energy consumption of each injection was estimated to be 40 J, which is negligible compared to the system overall energy consumption (25 W X 500 s = 12.5 kJ).

3.2.3. Detectors

A flow-through μPID (shown in Fig. 2C) was adapted from our previously reported version [15]. The dimensions of microfluidic channel were increased to 380 μm in width, 400 μm in depth, and 2.5 cm in length. Due to the wider channel width, the baseline signal was reduced. Because of the nondestructive nature of the μPID, the analytes eluted from the 1st-dimensional column can go through and be detected by the μPID before being routed to the next dimension. The μPID used in this study can provide sensitive detection (10's of picograms) of VOCs with the photoionization potential lower than 10.6 eV.

The μHDBD-PID (shown in Fig. 2D) installed in the 2nd-dimensional column was used to detect formaldehyde that has the photoionization potential of 10.88 eV. It was adapted from our previously reported version [16]. In the current version, the discharge electrodes distance was decreased to 580 μm, resulting in a lower plasma inducing voltage and power consumption. A home-made high-voltage high-frequency converter [16] with 1 V DC input and 1.2 kV @ 7.7 kHz output was used to drive helium plasma. The power consumption was estimated to be 90 mW. The details of the μHDBD-PID can be found in the Supplementary Information. The signals from both μPID and μHDBD-PID were acquired by a USB 6003 OEM analog input channel with a 10 Hz digital low pass filter.

3.2.4. Micro-Deans switch

The micro-Deans switch serves as a gas flow router in the device to control the gas flow through auxiliary gas. By switching the inlet of auxiliary gas through a miniaturized three-port valve, the upper stream flow can be directed to one of the outlets (see Fig. 3A). The flow channel of the micro-Deans switch had dimensions (150 μm wide and 380 μm deep) similar to a GC column. Therefore, the dead volume of the micro-Deans switch is negligible. Additionally, a buffer line connected to both auxiliary gas inlets can further reduce the dead volume in auxiliary gas inlets. In order to fully control the flow routing, the auxiliary gas pressure was required to be equal to (shown in Fig. 3B) or greater than the inlet pressure. The flow limitation/balance can simply be achieved by using flow resistors shown in Fig. S4A. Compared to an electric pressure controller, the flow resistor had significant advantages of low cost, low energy consumption, robustness, and size.

3.3. GC operation

The vapor was collected through a 20-cm long tubing by the preconcentrator at a sampling flow rate of 40 mL/min. The sampling time was adjustable and usually required a few minutes. After sampling the flow was switched to the carrier gas and run for 30 s for stabilization of the carrier gas. Then the preconcentrator was heated to inject the analytes into the 1st-dimensional column, which was preheated to 23 °C and initially connected with the waste line. The heart-cutting window was applied from 34 s to 50 s by the micro-Deans switch to send formaldehyde (along with other vapors within the window) to the thermal injector in front of the 2nd-dimensional column. Then the thermal injector was heated to inject the samples into the 2nd-dimensional column, which was maintained isothermally at 80 °C. The eluents from the 2nd-dimensional column were detected by the μHDBD-PID. Concomitant with the 2nd-dimensional separation, other analytes could continue to be separated by the 1-dimensional column and detected by the μPID. During the operation, the flow rate for the 1st- and 2nd-dimensional column was kept at 2 mL/min. The details of the gas flow layouts at sampling, 1st-dimensional separation, target cutting, and 1st- and 2nd-dimensional separation can be found in Fig. S5.

3.4. Sample preparation

Various concentrations of formaldehyde vapor were generated by the corresponding aqueous solutions. The vapor-liquid equilibrium is calculated by Eq. (1) [17]

$$[HCHO(aq)] = 10^{\left[\left(\frac{4538}{T}\right)-11.34\right]}[HCHO(g)]^{\left[\left(\frac{252.2}{T}\right)+0.2088\right]} \quad (1)$$

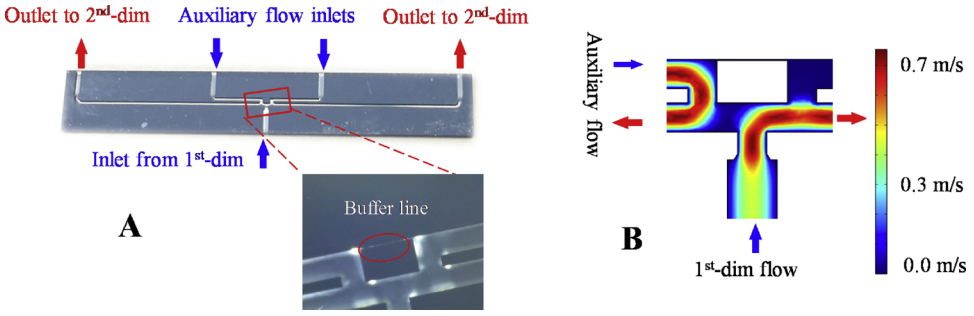

Fig. 3. (A) Picture of the micro-Deans switch and the enlarged buffer line area. (B) Fluidic simulation for the enlarged area in (A) by COMSOL Multiphysics® under the condition of equal inlet pressure on the auxiliary inlet and the 1st-dimensional inlet. It can be seen that the auxiliary flow and the 1st-dimensional flow are directed to the left and right outlet, respectively, without interfering with each other.

Table 1
Formaldehyde vapor volume concentrations and corresponding solution concentrations.

Vapor concentration ppb (V/V)	Solution concentration (μmol/L)
0.5	1.671
2	7.323
8	32.10
31.5	138.6
100	474.0

where $[HCHO(aq)]$ (M) is the formaldehyde molar concentration in water, T(K) is temperature (294 K), and $[HCHO(g)]$ (atm) is the formaldehyde vapor pressure. Based on the purge efficiency theory reported by Zhou et al. [18], the formaldehyde purge efficiency is almost zero due to the high Henry's constant (4415 mol L^{-1} atm^{-1}, which is converted from 32 mol m^{-3} Pa^{-1} at 298.15 K with temperature dependent constant of 6800 K) [19]. Therefore, we can assume the vapor-liquid equilibrium is always maintained during the experiments. Table 1 lists formaldehyde samples being tested in this work. The sample purge setup is shown in Fig. S6. A 20-mL sample vial filled with 10 mL of sample solution was sealed with a metal cap having a polytetrafluoroethylene septum. The purified air flowed into the vial at the flow rate of 40 mL/min. The relative humidity level at the outlet of the sample purge setup was measured to be 63%–65 % at 23 ℃ by a dew-point senor (see Fig. S7), slightly higher than the recommended indoor relative humidity level of 40–60%. The vapors were collected at the vial headspace and trapped by the preconcentrator.

4. Result and discussion

4.1. Formaldehyde retention time

Fig. 4A shows an exemplary 2nd-dimensional chromatogram for the VOCs cut from the window of 34 s to 50 s from the 1st-dimension separation. The formaldehyde retention time, which is defined as its peak position is 141.1 s with a full-width-at-half-maximum of 27.3 s. The formaldehyde retention statistics obtained from 15 measurements at various concentrations are summarized as a box plot in Fig. 4B. The average retention time is found to be 141.1 s with the standard deviation of only 0.2 s. The low retention time variation is due to the stable flow rate and the accurate temperature control in our device. The total assay time is less than 11 min, including < 6 min of sampling, < 1 min in 1st-dimensional separation and < 4 min in 2nd-dimensional separation.

4.2. Sampling time-dependent

As we discussed above, the liquid-vapor equilibrium is assumed to be maintained during the sampling process. To verify, the sampling time-dependent test was carried out by running 2 ppb (V/V) formaldehyde detection with 1 min, 2 min, 4 min, 6 min, and 8 min of sampling time. The result of formaldehyde peak area integrated from the 2nd-dimensional chromatogram *versus* sampling time was plotted in Fig. 5, showing excellent linear dependence. Therefore, the purging setup in Fig. S6, along with the purging parameters such as flow rate and sampling time, can provide a constant and accurate formaldehyde vapor concentration.

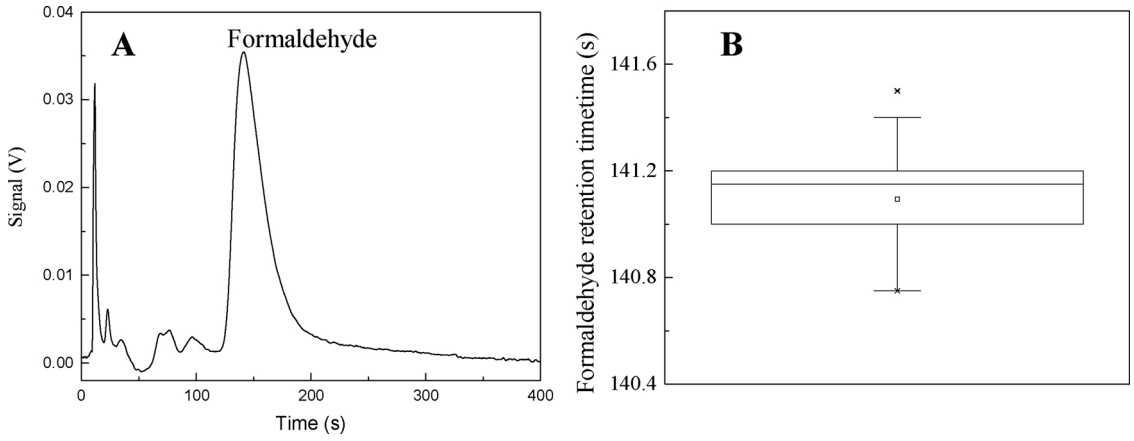

Fig. 4. (A) 2nd-dimensional chromatogram of VOCs cut from the window of 34 s to 50 s in the 1st-dimension. The formaldehyde (31.5 ppb) peak is located at 141.3 s with the full-width-at-half-maximum of 27.9 s. (B) Box plot of 15 measurements (3 measurements of vapor volume concentrations at 0.5 ppb, 2 ppb, 8 ppb, 31.5 ppb, and 100 ppb) of formaldehyde retention time in 2nd–dimensional separation with the maximum value of 141.5 s, the minimum value of 140.75 s, and the mean value at 141.1 s.

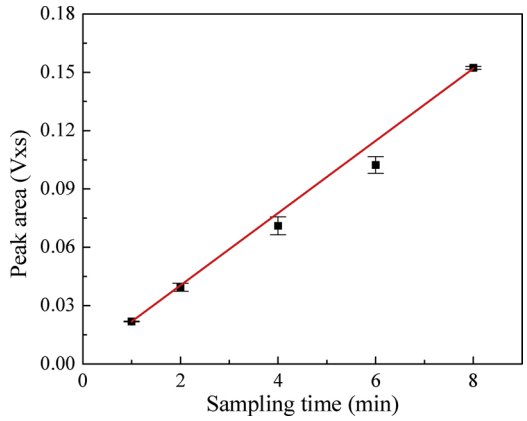

Fig. 5. Formaldehyde peek area in the 2nd-dimensional chromatogram as a function of different sampling times for 2 ppb (V/V) formaldehyde at the sample flow rate of 40 mL/min. The solid line is the linear fit with the slope of 0.01859, the intercept of 0.00322, and the R^2 value of 0.99958. The error bar for each data point was obtained from 3 measurements.

4.3. Linearity and sensitivity

The formaldehyde linearity and sensitivity characterization were carried out by testing samples listed in Table 1 with conditions described in the Methods section. The result shown in Fig. 6 was generated by integrating formaldehyde peak area in the 2nd-dimensional chromatogram. The error bar was calculated by solving the standard deviation of formaldehyde peek area in 3 repeated tests which shows an excellent linear response to vapor volume concentration ranging from 0.5 ppb to 100 ppb. The low detection limit (LOD) for 6 min of sampling was calculated to be 0.23 ppb (V/V) by Eq. (2).

$$LOD = \frac{3\sigma}{S} \quad (2)$$

where S (2.2 mV/ppb) is sensitivity at 0.5 ppb (V/V) test; σ (0.169 mV) is the standard deviation of the baseline noise. Given that the lowest regulated formaldehyde vapor concentration is 2 ppb (V/V) (see Table S1), our device can satisfactorily meet the current formaldehyde detection requirement (Fig. 6).

4.4. Simultaneous analysis of formaldehyde and other VOCs

In practice, such as indoor air analysis, other VOCs may need to be analyzed along with formaldehyde. Here, we demonstrate the capability of our device in simultaneous, rapid analysis of formaldehyde and BTEX (benzene, toluene, ethylbenzene, and p-xylene). In this case, formaldehyde was separated by the 1st- and 2nd-dimensional column and detected by μHDBD-PID, whereas BTEX separation was accomplished by temperature-ramping the 1st-dimensional column and detected by μPID. In the experiment, a mixture sample solution was prepared that contained formaldehyde (32.1 μmol/L), benzene (0.064 μmol/L), toluene (0.083 μmol/L), ethylbenzene (0.094 μmol/L), and p-xylene (0.094 μmol/L). The flow rate was still 40 mL/min and the sampling time was 6 min. From the previously published experimental results [18], the purge efficiency for BTEX was approximately 80%. Thus, the equivalent vapor volume concentrations of formaldehyde and BTEX were 8 ppb, 51 ppb, 70 ppb, 75 ppb, and 75 ppb, respectively. The representative chromatogram was presented in Fig. 7. The 1st-dimensional column temperature was initially maintained at 23 °C for 100 s and heated to 53 °C at a rate of 4.5 °C/min. The separation and detection of formaldehyde in the 2nd-dimensional column can be performed in parallel with the BTEX separation and detection in the 1st-dimensional column. The whole analysis time was only 14 min and can be further reduced by applying a more rapid temperature ramping profile.

5. Summary

We have developed and characterized the performance of a portable 2-D GC device based on heart-cutting technology for a sensitive, rapid, and on-site formaldehyde detection. The miniaturization of the GC components resulted in a compact size and light weight instrument. The test results of elution time, sampling time dependence, linearity, and sensitivity show that our portable 2-D GC system can carry out accurate and repeatable formaldehyde detection with a detection limit (at 3σ) of 0.23 ppb (V/V) with only 6 min of sampling time. The integration of open tubular column (for the 1st-dimension) and porous layer open tubular (PLOT) column (for the 2nd-dimension) provides a perfect solution for high volatile compounds separation, in which the heart-cutting from the 1st-dimensional separation avoids the potential contamination to the PLOT column by other VOCs having lower volatilities. In addition to formaldehyde, other commonly seen VOCs such as BTEX can be detected in short amount of time. We envision that the fully automated GC device demonstrated here will have a broad range of applications in continuous monitoring of air pollution and other toxic volatile materials.

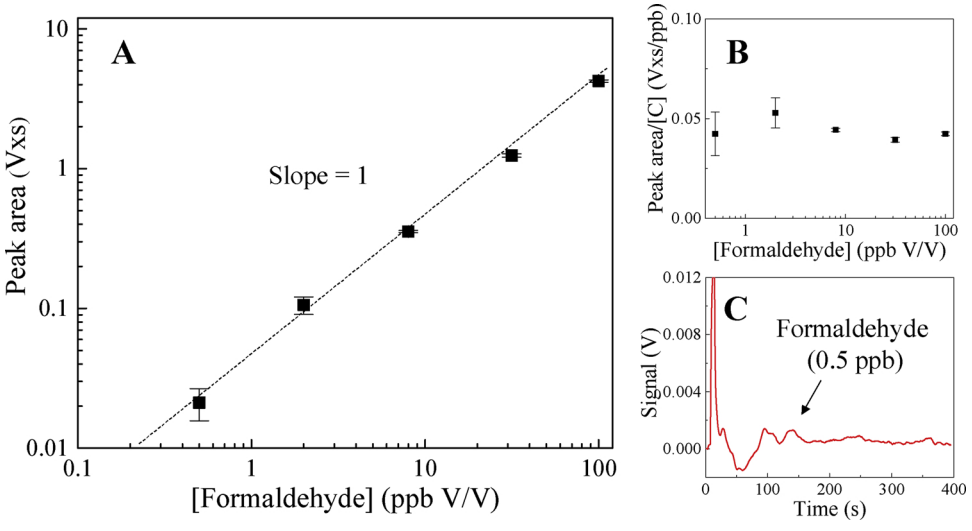

Fig. 6. Formaldehyde detection linearity and sensitivity test. (A) Peak area as a function of formaldehyde concentration in the log-log scale. The dashed lines show a linear curve with a unity slope to guide an eye. (B) Peak areas normalized to the corresponding concentration *versus* formaldehyde concentration. (C) A representative 2nd-dimensional chromatogram for 0.5 ppb formaldehyde. In all measurements, the sampling time was kept at 6 min. The error bar for each data point was obtained from 3 measurements.

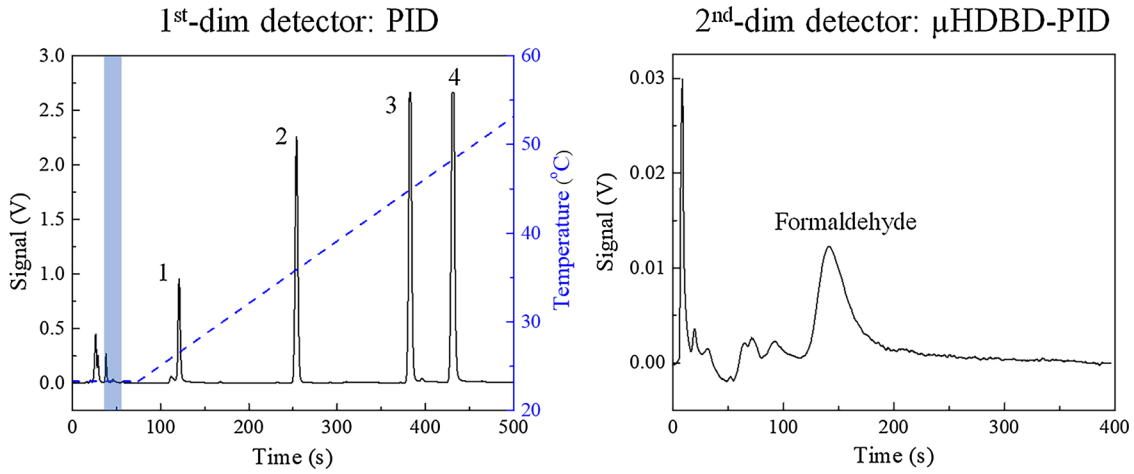

Fig. 7. (A) 1st-dimensional separation and detection result for formaldehyde and BTEX (1: benzene; 2: toluene; 3: ethylbenzene, and 4: p-xylene). The formaldehyde heart-cutting window is represented by the shaded area. The dashed blue curve shows the temperature ramping profile (T = 23 °C for 100 s and then to 53 °C at a rate of 4.5 °C/min). (B) 2nd-dimensional chromatogram of VOCs cut out from 1st-dimension. The 2nd-dimensional column was maintained isothermally at 80 °C. The flow rate for both columns was kept at 2 mL/min (For interpretation of the references to colour in this figure legend, the reader is referred to the web version of this article).

Acknowledgements

We would like to acknowledge the support from IARPA (contract #: FA8650-17-C-9106) and Nanova Environmental, Inc. and the assistance from Lurie Nanofabrication Facilities at the University of Michigan Ann Arbor during microfabrication of the GC components.

Appendix A. Supplementary data

Supplementary material related to this article can be found, in the online version, at doi:https://doi.org/10.1016/j.snb.2018.11.156.

References

[1] S.K. Brown, M.R. Sim, M.J. Abramson, C.N. Gray, Concentrations of volatile organic compounds in indoor air – a review, Indoor Air 4 (2) (1994) 123–134.
[2] A. Blondel, H. Plaisance, Screening of formaldehyde indoor sources and quantification of their emission using a passive sampler, Build. Environ. 46 (6) (2011) 1284–1291.
[3] K.C. Gupta, A.G. Ulsamer, P.W. Preuss, Formaldehyde in indoor air: sources and toxicity, Environ. Int. 8 (1) (1982) 349–358.
[4] R.A. Squire, L.L. Cameron, An analysis of potential carcinogenic risk from formaldehyde, Regul. Toxicol. Pharmacol. 4 (2) (1984) 107–129.
[5] P.-R. Chung, C.-T. Tzeng, M.-T. Ke, C.-Y. Lee, Formaldehyde gas sensors: a review, Sensors 13 (4) (2013) 4468–4484.
[6] R.K. Beasley, C.E. Hoffmann, M.L. Rueppel, J.W. Worley, Sampling of formaldehyde in air with coated solid sorbent and determination by high performance liquid chromatography, Anal. Chem. 52 (7) (1980) 1110–1114.
[7] N. Sugaya, T. Nakagawa, K. Sakurai, M. Morita, S. Onodera, Analysis of aldehydes in water by head space-GC/MS, J. Health Sci. 47 (1) (2001) 21–27.
[8] M.-A. del Barrio, J. Hu, P. Zhou, N. Cauchon, Simultaneous determination of formic acid and formaldehyde in pharmaceutical excipients using headspace GC/MS, J. Pharm. Biomed. Anal. 41 (3) (2006) 738–743.
[9] S. Belman, The fluorimetric determination of formaldehyde, Anal. Chim. Acta 29 (1963) 120–126.
[10] A.T. Güntner, V. Koren, K. Chikkadi, M. Righettoni, S.E. Pratsinis, E-Nose sensing of low-ppb formaldehyde in gas mixtures at high relative humidity for breath screening of lung cancer? ACS Sens. 1 (5) (2016) 528–535.
[11] X. Wang, Y. Si, J. Wang, B. Ding, J. Yu, S.S. Al-Deyab, A facile and highly sensitive colorimetric sensor for the detection of formaldehyde based on electro-spinning/netting nano-fiber/nets, Sens. Actuators B Chem. 163 (1) (2012) 186–193.
[12] X. Yang, Y. Wang, W. Liu, Y. Zhang, F. Zheng, S. Wang, D. Zhang, J. Wang, A portable system for on-site quantification of formaldehyde in air based on G-quadruplex halves coupled with A smartphone reader, Biosens. Bioelectron. 75 (2016) 48–54.
[13] K. Toda, W. Tokunaga, Y. Gushiken, K. Hirota, T. Nose, D. Suda, J. Nagai, S.-I. Ohira, Mobile monitoring along a street canyon and stationary forest air monitoring of formaldehyde by means of a micro-gas analysis system, J. Environ. Monit. 14 (5) (2012) 1462–1472.
[14] Y. Suzuki, N. Nakano, K. Suzuki, Portable sick house syndrome gas monitoring system based on novel colorimetric reagents for the highly selective and sensitive detection of formaldehyde, Environ. Sci. Technol. 37 (24) (2003) 5695–5700.
[15] H. Zhu, R. Nidetz, M. Zhou, J. Lee, S. Buggaveeti, K. Kurabayashi, X. Fan, Flow-through microfluidic photoionization detectors for rapid and highly sensitive vapor detection, Lab Chip 15 (14) (2015) 3021–3029.
[16] H. Zhu, M. Zhou, J. Lee, R. Nidetz, K. Kurabayashi, X. Fan, Low-power miniaturized helium dielectric barrier discharge photoionization detectors for highly sensitive vapor detection, Anal. Chem. 88 (17) (2016) 8780–8786.
[17] S. Dong, P.K. Dasgupta, Solubility of gaseous formaldehyde in liquid water and generation of trace standard gaseous formaldehyde, Environ. Sci. Technol. 20 (6) (1986) 637–640.
[18] M. Zhou, J. Lee, H. Zhu, R. Nidetz, K. Kurabayashi, X. Fan, A fully automated portable gas chromatography system for sensitive and rapid quantification of volatile organic compounds in water, RSC Adv. 6 (55) (2016) 49416–49424.
[19] R. Sander, Compilation of Henry's law constants (version 4.0) for water as solvent, Atmos. Chem. Phys. 15 (8) (2015).